

Design of Back-Stepping Reaching Law Controller for Ultrasonic Motor Using Friction Drive

Gang-Feng Yan^{*,**}

Keywords : ultrasonic motor, back-stepping control, reaching law, PID control.

ABSTRACT

As the actuator of the control system, the ultrasonic motor is widely used in precision-manufactured drive equipment. In this paper, an approximate time-domain mathematical model is established firstly for the selected ultrasonic motor control system, and the parameters of the system models are identified using the least square method. Then, a back-stepping reaching law controller is proposed and designed for the selected ultrasonic motor system, the stability of the ultrasonic motor control system is proved, and the parameter selection method of the designed controller is given. Finally, the proportional integral derivative (PID) control method with large gain and the designed control method are used to track the same position signal, and a better control effect is achieved. The results show that for a position signal with a tracking amplitude of 40 mm, the PID control method has a maximum tracking error of 0.1362 mm, and the maximum tracking error of the back-stepping reaching law control method is 0.0816 mm. Under the same control parameters, after adding a load of 0.3 kg, the maximum tracking errors of the PID control method and the back-stepping reaching law control method are 0.1519 mm and 0.0892 mm respectively. The proposed control method is easy to implement in engineering, and the control method requires few parameters to be adjusted and is easy to adjust, therefore, it has good engineering application value.

*Paper Received May, 2023. Revised November, 2023. Accepted December, 2023. Author for Correspondence: Gang-Feng Yan.
Email: yangangfeng@cdu.edu.cn*

** Associate Professor, Department of Automation, College of Electronic Information and Electrical Engineering, Chengdu University, Chengdu 610106, PR China.*

*** Visiting Researcher, Key Laboratory of Advanced Manufacturing Technology, Ministry of Education, Guizhou University, Guiyang 550025, PR China.*

INTRODUCTION

With the continuous advancement of science and technology, many technical fields have higher and higher requirements for high-precision positioning systems. Whether it is biological engineering, medical engineering, integrated circuits, or aerospace, optical fiber transmission, etc., the demand for micron-level precision positioning and drive control technology is extremely urgent (Lu et al., 2017; Ng et al., 2019; Xiao et al., 2016; Corapsiz et al., 2016; Lehmann et al., 2018; Mohammed et al., 2020). The traditional electromagnetic mutual induction motor has complex structure, large volume and poor positioning accuracy, which is difficult to meet the needs of the above-mentioned fields. As a friction-coupled piezoelectric actuator, the ultrasonic motor uses the inverse piezoelectric effect of piezoelectric materials to convert electrical energy into mechanical energy, and through the friction between the mechanical structures, the reciprocating micro-amplitude motion of the elastic body is converted into macroscopic linear motion of the motion platform. Ultrasonic motor has a very compact structure, small inertia of the moving body, fast response braking, and can directly drive the load. It has the characteristics of low speed and high torque, and is the first choice for realizing micro-level precise positioning.

The inherent nonlinear characteristics and complex frictional transmission behavior of ultrasonic motors are the biggest challenges in the modeling and control of ultrasonic motors. PID control is by far the most common control method. Most feedback loops use this method to control. PID controller and its improved type are the most common controllers in industrial process control, but PID control technology is difficult to achieve good expected control effect in complex nonlinear systems.

In order to improve the control effect of the control system, many scholars have tried many advanced control strategies to improve the performance of the complex control system. For repetitive displacement tracking tasks, iterative learning control can be used to achieve high-precision

control (Yan et al., 2019). Iterative learning control obtains the control input that can produce the desired output trajectory by repeatedly applying the information obtained from the previous experiments, so as to improve the control quality. The disadvantage of iterative learning control is that it has higher requirements on the initial conditions of the system, and the robustness of the control algorithm is poor. For the vast majority of non-repetitive displacement tracking tasks, a series of feedback control schemes have been proposed for high-precision tracking of ultrasonic motors, such as sliding mode control (Safa et al., 2018; Yan, 2022; Yan, 2022; Liang et al., 2022), fuzzy control (Bani Melhem et al., 2020; Shi et al., 2020), adaptive control (Zhou et al., 2020; Motoi et al., 2020; Yan, 2022), neural network control (Li et al., 2020; Yan, 2021; Napole et al., 2021), and H^∞ control (Sebastian et al., 2005; Napole et al., 2021), etc. The control algorithm proposed in reference (Safa et al., 2018) generates the control signal by estimating the upper bound of the uncertainty (disturbance) of the system, and converts the discontinuous sign function into the time derivative of the control input signal, and then integrates to obtain the continuous control signal to reduce chattering caused by control. Reference (Yan, 2022) does not use the sign function to directly produce the control effect, but introduces the PID operation of the sliding mode surface to force the system to move toward the sliding mode surface, so that the control system exhibits the robustness of sliding mode control to un-modeled dynamics. In order to improve the control effect, the effectiveness of sliding mode control can also be improved by establishing compensation of the system model (Yan, 2022). Reference (Liang et al., 2022) proposes a method that uses a nominal model to construct a nonlinear sliding mode surface, and designs a nonlinear sliding mode controller through coordinated adjustment of the frequency and amplitude of the two-phase drive control voltage. For the system composed of linear motor and piezoelectric actuator, Reference (Bani Melhem et al., 2020) selects the position and speed of piezoelectric actuator as the fuzzy input of the fuzzy control system, and the fuzzy output is the speed of the linear motor, thereby, a better control effect is obtained. Reference (Shi et al., 2020) utilizes the nonlinear input-output mapping capability of fuzzy logic to realize nonlinear variable-parameter PID control. Reference (Zhou et al., 2020) proposes a model, which series Bouc-Wen model and linear dynamic model, to describe the rate-dependent hysteresis characteristics of the piezoelectric micro-positioning platform, and designs a model reference adaptive controller based on inverse model compensation for piezoelectric micro-positioning platform. Reference (Motoi et al., 2020) uses a recursive least squares algorithm to estimate the relevant model parameters in real time,

thereby constituting an adaptive control signal. Reference (Yan, 2022) designed a continuous switching adaptive sliding mode controller by defining double sliding mode surfaces to form a sliding mode sector, and applied the controller to the control of an ultrasonic motor system, although the introduction of the sliding mode sector can fundamentally avoid the chattering of the system by properly selecting the control parameters, the control accuracy still needs to be improved, for a position signal with a tracking amplitude of 35 mm, the maximum tracking error of the continuous switching adaptive sliding mode control is 0.1589 mm. Reference (Li et al., 2020) describes piezoelectric actuators as nonlinear equations with two unknown variables, then, the neural network self-tuning control is realized by using the approximation and adaptive parameter adjustment ability of the neural network. In the process of modeling a neural network for piezoelectric actuators, Reference (Yan, 2021) found that over-fitting can be avoided by identifying the main input variables and using them only as inputs to the neural network, unlike most neural network lag models, using a simple static feed-forward neural network, which does not require complex lag operators, can greatly simplify the implementation of piezoelectric actuator inverse systems. Reference (Napole et al., 2021) uses a hyper-twist algorithm combined with an artificial neural network to design a controller, which reduces the motion error of piezoelectric actuators compared to PID controller. Reference (Sebastian et al., 2005) employs a robust linear controller to handle the nonlinear and changing bending dynamics associated with piezoelectric actuation. For piezoelectric actuators, Reference (Napole et al., 2021) uses artificial neural network feed-forward to model the nonlinearity of the system, closed-loop compensator to reduce un-modeled dynamics, uncertainties and disturbances, and then adjusts the control parameters online through specific indicators, in the tracking effect, its performance is better than the traditional PID controller. These control schemes can achieve acceptable tracking accuracy and interference suppression performance, but the control laws used are quite complex, and the accuracy of the system model is also required. In addition, there are also reference (Khalil et al., 2023) that use a model-free, real-time adaptive extreme value search controller to continuously determine the optimal driving frequency of the ultrasonic motor to achieve a control effect with minimal steady-state error. Iterative learning control is introduced into the real-time adjustment of PI controller parameters to obtain better control performance (Lu et al., 2023). For friction transmission type ultrasonic motors, reference (Zhao et al., 2023) proposes a temperature drift maximum efficiency point tracking control method by analyzing the relationship between the maximum efficiency point and the drive circuit

voltage and frequency in order to compensate for the impact of temperature on the operating efficiency of the ultrasonic motor.

The back-stepping control method decomposes the complex nonlinear system into multiple simpler and lower-order systems for control by introducing virtual control, ensures the stability of the system by selecting the appropriate Lyapunov function, and gradually derives the final control law to achieve effective control of the system. The general design method of back-stepping control has high requirements on the accuracy of the system model, and the control accuracy is easily affected by parameter uncertainty and unknown external disturbance. Based on this, this paper proposes to introduce a modified reaching law to design a back-stepping controller. The controller is designed by defining a state variable containing a virtual control signal. The designed back-stepping reaching law controller has fewer parameters and is easy to adjust. For the control of the same tracking task, the control effects of the PID controller and the back-stepping reaching law controller proposed in this paper are compared. The results show that the back-stepping reaching law controller has no chattering and is more accurate than the PID controller. Therefore, it has good engineering application value in driving and controlling precision equipment.

This paper is organized as follows. The experimental equipment and dynamic modeling are introduced in section 2, in section 3, the design method of the back-stepping reaching law controller and test results of the control system are given, conclusions are given in section 4.

EXPERIMENTAL EQUIPMENT AND DYNAMIC MODELING

In this paper, the linear ultrasonic motor control system platform used for research is shown in Fig. 1. Its maximum motion travel is 120 mm and its maximum velocity is 220 mm/s (Parker Ltd, 2012). The ultrasonic motor system is equipped with a piezoelectric driver, which model is AB1A Driver from Nanomotion company, integrated into the system. Renishaw RGB25Y encoder with a resolution of 0.1 μ m (RGB25Y Company, 2011) is used as the position feedback sensor. On the host computer containing the dSPACE DS1104 card, MATLAB is used to realize the programming of the control law. The DS1104 card is an integrated control board containing A/D conversion and D/A conversion, which can be used to quickly control prototype verification functions. The sampling period used in this paper is 0.0001 s. The software used in the user operation interface is dSPACE Control Desk, which is used for real-time adjustment of parameters and real-time measurement of data.

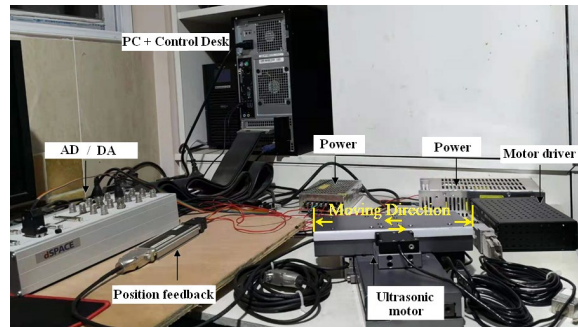


Fig. 1. Ultrasonic motor control system.

The working principle of the ultrasonic motor control system is to use the inverse piezoelectric effect of piezoelectric ceramics. After inputting the driving voltage to the linear ultrasonic motor, the piezoelectric ceramics in the ultrasonic motor will produce inverse piezoelectric phenomenon, resulting in longitudinal and lateral bending. Through the deformation of the ceramic fingertips, high-frequency alternating vibrations are generated through the connected ceramic fingertips, and then, the worktable is driven by the friction between the ceramic fingertips and the drive belt to achieve linear motion (Yan, 2022).

In the process of determining the system model, first design a slow triangular wave signal input signal on the ultrasonic motor, and generates low-speed movement at a very low acceleration. In this way, the role of input force is only used to overcome the friction of ultrasonic motors. The experimental results can be obtained as shown in Fig. 2.

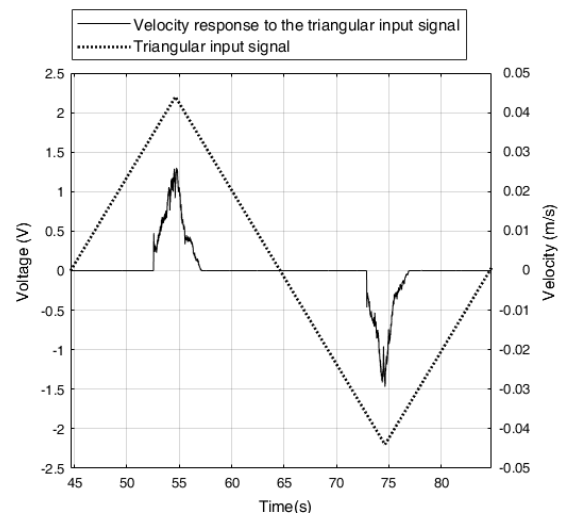


Fig. 2. Experimental results of force and response velocity.

It can be seen from Fig. 2 that the static friction force, Coulomb friction force and viscous friction force need to be considered. The speed of the ultrasonic motor is very small, and the coefficient of friction of air against solids is also very small, so in this case, we can ignore the drag friction force.

Note that the friction coefficient of the forward and backward direction of the ultrasonic motor is different. Considering static friction force, Coulomb friction force and viscous friction force, the dynamic characteristics of ultrasonic motors can be described by Newton's second law through the second-order differential equation with quality normalization as follows.

$$\ddot{x}(t) = -\frac{k_1}{m}\dot{x}(t) - \frac{k_2}{m}\text{sgn}(\dot{x}(t)) - \frac{1}{m}F_s + \frac{k_3}{m}u_1(t) \quad (1)$$

where, k_1 is the coefficient of viscous friction force, k_2 is the Coulomb friction force, $\text{sgn}(\dot{x}(t)) = \begin{cases} 1, \dot{x}(t) > 0 \\ 0, \dot{x}(t) = 0 \\ -1, \dot{x}(t) < 0 \end{cases}$, m denotes the rotor mass of

ultrasonic motor, F_s denotes the static friction force, k_3 represents constants of the voltage to force conversion, $u_1(t)$ is the control signal, in order to facilitate writing, let

$$a_1 = \frac{k_1}{m} = \begin{cases} a_{1p}, & \dot{x} > 0 \\ a_{1n}, & \dot{x} < 0 \end{cases} \quad (2)$$

$$a_2 = \frac{k_2}{m} = \begin{cases} a_{2p}, & \dot{x} > 0 \\ a_{2n}, & \dot{x} < 0 \end{cases} \quad (3)$$

$$a_3 = \frac{k_3}{m} \quad (4)$$

a_3 represents the conversion constant of voltage to force, $a_3 = 3 \text{ N}/(\text{v.kg})$, which is provided in the linear ultrasonic motor product documentation (Parker Ltd, 2012). In order to obtain the values of the remaining parameters in the model (1), Considering the pulse width signal with a large amount of amplitude in the system, which can minimize the impact of static friction on the system.

Therefore, By using a pulse input of 0.4 s duration and with 2.9 V, -2.9 V of amplitude, the velocity response to the pulse inputs is obtained as shown in Fig. 3.

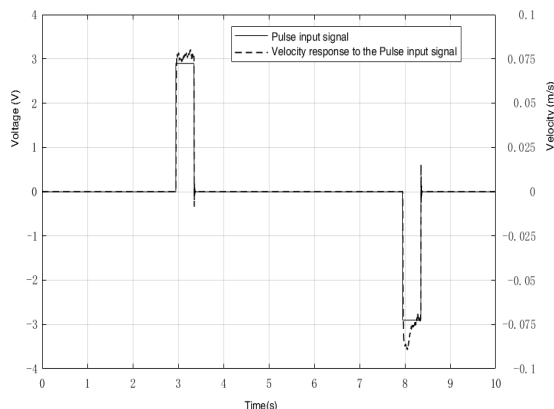


Fig. 3. Pulse input of 0.4s duration and with ± 2.9 V of amplitude and its velocity response.

Through experiments, the following equation can be obtained

$$\begin{cases} 0.07694a_{1p} + a_{2p} - 3 \times 2.9 = 0 \\ -0.07636a_{1n} - a_{2n} + 3 \times 2.9 = 0 \end{cases} \quad (5)$$

Use similar experiments, using a pulse of 0.4 s duration and amplitudes of 2.3 V, 2.4 V, 2.5 V, 2.7 V, 2.8 V, 2.0 V, 3.1 V, -2.4 V, -2.6, -2.6 V, -2.7 V, -2.8 V, -2.9 V, -3.0 V, -3.1 V respectively, the following results can be obtained.

$$\begin{bmatrix} 0 & 0.02703 & 0 & 1 \\ 0 & 0.03295 & 0 & 1 \\ 0 & 0.03989 & 0 & 1 \\ 0 & 0.05509 & 0 & 1 \\ 0 & 0.06589 & 0 & 1 \\ 0 & 0.07694 & 0 & 1 \\ 0 & 0.08838 & 0 & 1 \\ 0 & 0.10371 & 0 & 1 \\ -0.03209 & 0 & -1 & 0 \\ -0.03715 & 0 & -1 & 0 \\ -0.04324 & 0 & -1 & 0 \\ -0.05184 & 0 & -1 & 0 \\ -0.06481 & 0 & -1 & 0 \\ -0.07636 & 0 & -1 & 0 \\ -0.08908 & 0 & -1 & 0 \\ -0.10545 & 0 & -1 & 0 \end{bmatrix} \cdot \begin{bmatrix} a_{1n} \\ a_{1p} \\ a_{2n} \\ a_{2p} \end{bmatrix} = \begin{bmatrix} 2.3 \\ 2.4 \\ 2.5 \\ 2.7 \\ 2.8 \\ 2.9 \\ 3.0 \\ 3.1 \\ -2.4 \\ -2.5 \\ -2.6 \\ -2.7 \\ -2.8 \\ -2.9 \\ -3.0 \\ -3.1 \end{bmatrix} \quad (6)$$

Let the above equation correspond to $X \cdot A = Y$, We use e to denote the difference between Y and $X \cdot A$, define $E = e^T e$, Using the least-squares method, by using

$$A = (X^T X)^{-1} X^T Y \quad (7)$$

$a_{1n}, a_{1p}, a_{2n}, a_{2p}$ can be obtained, by solving the equation (7), as

$$\begin{bmatrix} a_{1n} \\ a_{1p} \\ a_{2n} \\ a_{2p} \end{bmatrix} = \begin{bmatrix} 27.6684 \\ 31.3938 \\ 6.5207 \\ 6.2151 \end{bmatrix} \quad (8)$$

Using equation (1), while ignoring static friction, contrasting curves for velocities are obtained as a response to the pulses of amplitude 3.1 V and -3.1 V, as shown in Fig. 4. In Fig. 4, the dotted line shows the response of the equation (1) while the solid line shows the response of the actual system.

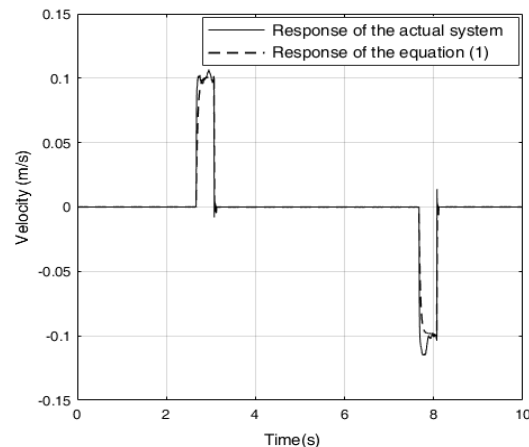


Fig. 4. Pulse width signal input with 0.4s duration and ± 3.1 V amplitude pulse, the response curve of model (1) and the measured output of the system.

Because it is difficult to simulate the static friction, the velocity of the system at this time is zero. According to the result of the Fig. 4, It can be seen that the simulation results are relatively close to the actual system results, so the model can be used to design the control system as follows.

$$\dot{x}(t) = -a_1\dot{x}(t) - a_2 \operatorname{sgn}(\dot{x}) + 3u_1(t) \quad (9)$$

The values of a_1 and a_2 are

$$a_1 = \begin{cases} 31.3938 & \dot{x}(t) > 0 \\ 27.6684 & \dot{x}(t) < 0 \end{cases} \quad (10)$$

$$a_2 = \begin{cases} 6.2151 & \dot{x}(t) > 0 \\ 6.5207 & \dot{x}(t) < 0 \end{cases} \quad (11)$$

The actual control system can be expressed as

$$\ddot{x}(t) = -a_1\dot{x}(t) - a_2 \operatorname{sgn}(\dot{x}(t)) - f_d(t) + u(t) \quad (12)$$

where, $f_d(t)$ represents un-modeled dynamics and disturbances to the system, $u(t) = 3u_1(t)$. In order to write, the time variable t is omitted in the following derivation process.

CONTROL METHOD DESIGN AND TESTING

First, the position signal to be tracked is shown in Fig. 5.

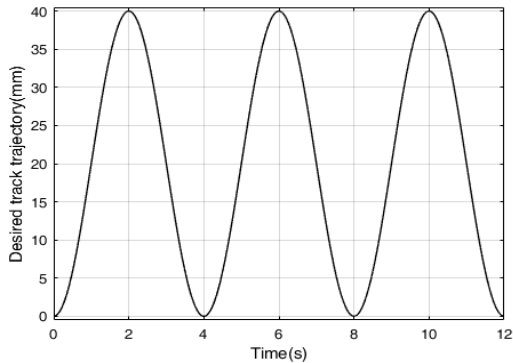


Fig. 5. Desired tracking signal.

The state variables v_1, v_2 are defined as follows

$$v_1 = x_d - x \quad (13)$$

$$v_2 = \dot{x}_d - \dot{x} + bv_1 \quad (14)$$

where, x_d denotes desired track trajectories, b is a parameter to be designed which is greater than 0.

In the (v_1, v_2) coordinates, the system can be expressed as

$$\begin{cases} \dot{v}_1 = -bv_1 + v_2 \\ \dot{v}_2 = \ddot{x}_d + a_1\dot{x} + a_2 \operatorname{sgn}(\dot{x}) + f_d - 3u + bv_1 \end{cases} \quad (15)$$

In the equation $\dot{v}_1 = -bv_1 + v_2$, considering v_2 as a virtual control signal, this equation can be rewritten as

$$\dot{v}_1 = -bv_1 + w \quad (16)$$

which is a first order linear system with w as a control input signal.

To stabilize the state variable v_1 , we consider the candidate Lyapunov function

$$V_1(v_1) = \frac{1}{2}v_1^2 \quad (17)$$

Clearly, V_1 is positive definite. Taking the derivative of V_1 , we can get

$$\dot{V}_1(v_1) = v_1(-bv_1 + w) \quad (18)$$

Select the virtual controller $w = -cv_1$, the above equation becomes $\dot{V}_1(v_1) = -(b+c)v_1^2$, which is negative definite.

So, according to Lyapunov stability theory, the closed-loop system

$$\dot{v}_1 = -(b+c)v_1 \quad (19)$$

is globally asymptotically stable.

In order for the state v_1 to be globally asymptotically stable with the desired dynamic performance as in equation, here choose $b+c=4$, the state v_2 must be equal to the virtual controller w . There is an error between v_2 and w . In order to make v_2 fast track w , the following state variable is defined

$$\xi = v_2 - w = v_2 + cv_1 \quad (20)$$

When $\xi \rightarrow 0$, choose $c=3$.

In the (v_1, ξ) coordinates, the control system can be expressed as

$$\begin{cases} \dot{v}_1 = \xi - (b+c)v_1 \\ \dot{\xi} = \ddot{x}_d + a_1\dot{x} + a_2 \operatorname{sgn}(\dot{x}) + f_d - 3u + (b+c)v_1 \end{cases} \quad (21)$$

In order to stabilize the state variable ξ , we consider the candidate Lyapunov function

$$V_2(\xi) = \frac{1}{2}\xi^2 \quad (22)$$

In order to satisfy the condition of Lyapunov stability, choose the following reaching law

$$\dot{\xi} = -d\xi - k\operatorname{sgn}(\xi) \quad (23)$$

Where, both d and k are parameters greater than 0 to be designed. considering that the function $\operatorname{sgn}(\xi)$ will cause chattering (Gao, 1996), it will seriously affect the service life of the ultrasonic motor system. Therefore, it is proposed to modify the function $\operatorname{sgn}(\xi)$ to $\frac{e^{1000\xi} - e^{-1000\xi}}{e^{1000\xi} + e^{-1000\xi}}$, so that the modified reaching law is

$$\dot{\xi} = -d\xi - k \frac{e^{1000\xi} - e^{-1000\xi}}{e^{1000\xi} + e^{-1000\xi}} \quad (24)$$

When ξ is very small and the phase trajectory is close to the switching surface $\xi \approx 0$, there is

$$\begin{cases} \dot{\xi} \approx -k & \xi > 0 \\ \dot{\xi} \approx k & \xi < 0 \end{cases} \quad (25)$$

Then we can made $\dot{V}_2(\xi)$ to be negative definite. Thus making ξ to be globally asymptotically stable.

The parameter k represents the switching speed when ξ reaches the switching surface $v_2 + cv_1 = 0$.

As long as k is small enough, the distance through the switching surface $v_2 + cv_1 = 0$ can be made small enough, so that the performance of the control system can be improved. Combined with equation (24), it can be seen that to ensure the fast approach to the switching surface $v_2 + cv_1 = 0$, the parameter d should take a large value, and k should take a small enough value.

Therefore, the back-stepping reaching law controller is designed as

$$u(t) = \frac{1}{3} \left(\ddot{x}_d + a_1 \dot{x} + a_2 \operatorname{sgn}(\dot{x}) + (b+c)\dot{v}_1 + d\xi + k \frac{e^{1000\xi} - e^{-1000\xi}}{e^{1000\xi} + e^{-1000\xi}} \right) \quad (26)$$

As a comparison, PID control is used to test the tracking performance of the ultrasonic motor under the same conditions. The parameters of PID control are Proportional coefficient is 10900, Integral coefficient is 830 and Derivative coefficient is 22, we adjust and select the parameters of PID control based on the tracking error is minimal under the condition of not leading to oscillatory output. According to the parameter adjustment method given in the design part of the back-stepping reaching law controller, the control parameters of the back-stepping reaching law controller are designed as $d = 262$, $k = 3$ by online adjustment. The tracking error results of the two control methods are shown in Fig. 6. The comparison of the maximum errors of the two control methods without load is shown in Table 1.

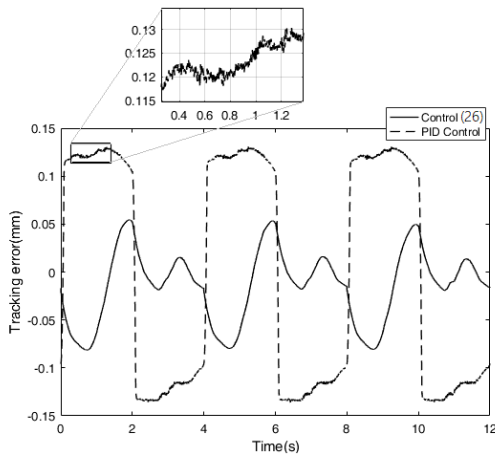


Fig. 6. Tracking error of PID controller and control method (26).

Table 1. Comparison of the maximum error of the two control methods without load.

Control Method	Maximum Error (mm)
PID Control	0.1362
Control Method (26)	0.0816

It can be seen that the tracking error of the control method (26) is significantly smaller than the tracking error of the PID controller, at the same time,

the system using back-stepping reaching law controller has no chattering, while the system using PID controller has obvious chattering, which can seriously affect the service life of the equipment, especially for precision motion equipment. The state variable ξ and its derivative $\dot{\xi}$ is shown in Fig. 7.

It can be seen that ξ and $\dot{\xi}$ are well convergent in the phase plane, which indicates that the control system is stable.

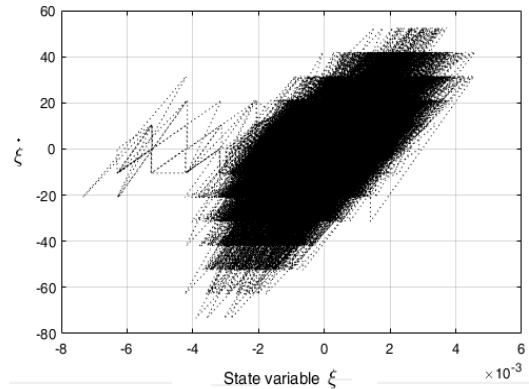


Fig. 7. ξ versus $\dot{\xi}$ on the phase plane.

Finally, to illustrate the robustness of the proposed back-stepping reaching law controller, an additional load of 0.3 kg was added to the ultrasonic motor control system, and the tracking error test was carried out under the condition that the control parameters of both control methods were kept unchanged. Fig. 8 shows the tracking error curves with additional load of 0.3 kg. The comparison of the maximum errors of the two control methods with additional load of 0.3 kg is shown in Table 2. It can be seen that both control methods have good robustness. It can be seen from Fig. 8 that the system using the back-stepping reaching law controller remained chatter free, while the chattering of the system with PID control is exacerbated.

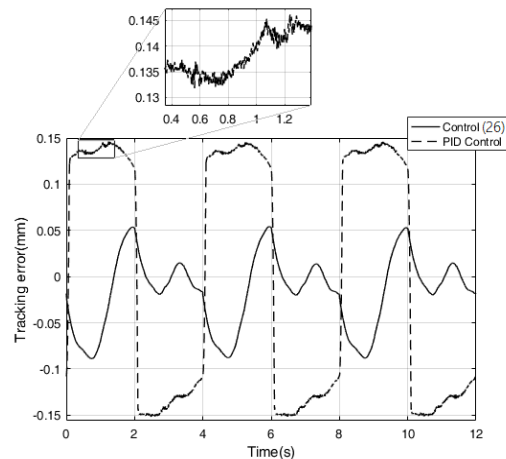


Fig. 8. Tracking error of PID controller and control method (26) with 0.3 kg load.

Table 2. Comparison of the maximum error of the two control methods with 0.3 kg load.

Control Method	Maximum Error (mm)
PID Control	0.1519
Control Method (26)	0.0892

The state variable ξ and its derivative $\dot{\xi}$ under additional 0.3 kg load are shown in Fig. 9. It can be seen that state variable ξ and its derivative $\dot{\xi}$ are still well converged on the phase plane.

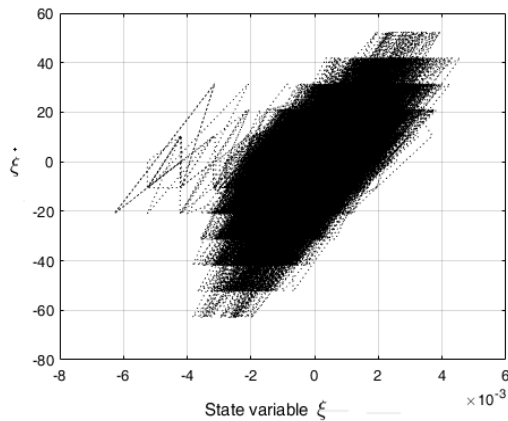


Fig. 9. ξ versus $\dot{\xi}$ on the phase plane with 0.3 kg load.

CONCLUSION

In this paper, the pulse width impulse response experiment is used to model the ultrasonic motor system, and then, based on this model, state variables containing virtual control variables are defined to describe the ultrasonic motor system, by introducing the modified reaching law, the back-stepping reaching law control algorithm of the ultrasonic motor is gradually derived. Using the Lyapunov stability analysis method, it is demonstrated that the tracking error of the defined state variables converges to zero asymptotically. Then the PID control and the designed back-stepping reaching law control are respectively applied to the tracking control tasks of the same ultrasonic motor. The results show that the back-stepping reaching law control can not only achieve better tracking control than PID control, but also has strong robustness under additional 0.3 Kg load.

ACKNOWLEDGMENT

Financial support for this work was provided by the Open Research Project of Key Laboratory of Advanced Manufacturing Technology, Ministry of Education (Guizhou University) (no. GZUAMT2021KF06).

REFERENCES

- Lu, Y., Zhang, C., Song, S., and Meng, M. Q. H., "Precise motion control of concentric-tube robot based on visual servoing," *2017 IEEE International Conference on Information and Automation (ICIA)*, IEEE, (2017).
- Ng, C., Liang, W., Gan C W, et al. "Precision motion control using nonlinear contact force model in a surgical device," *2019 41st Annual International Conference of the IEEE Engineering in Medicine and Biology Society (EMBC)*, IEEE, (2019).
- Xiao, B. S., Yin, and Kaynak, O., "Tracking control of robotic manipulators with uncertain kinematics and dynamics," *IEEE Trans. Ind. Electron.*, Vol.63, No.10, pp.6439-6449(2016).
- Corapsiz, M. F., and Erenturk, K., "Trajectory tracking control and contouring performance of three-dimensional CNC," *IEEE Trans. Ind. Electron.*, Vol.63, No.4, pp.2212-2220(2016).
- Lehmann, F., and Frignac, Y., "Performance analysis of a new calibration method for fiber nonlinearity compensation," *IEEE Commun. Lett.*, Vol.22, No.6, pp.1176-1179(2018).
- Mohammed, A. H., Raad, M. K., and Ammar, H. A., "The Method Of Calibration Compensation For Fiber Nonlinearity-A Review," *2020 International Congress on Human-Computer Interaction, Optimization and Robotic Applications (HORA)*, IEEE, (2020).
- Yan, G.F., Fang, H., and Meng, F., "High accuracy tracking of piezoelectric positioning stage by using iterative learning controller plus PI control," *Journal of the Brazilian Society of Mechanical Sciences and Engineering*, Vol.41, No.10, pp.1-9(2019).
- Safa, A., Abdolmalaki, R. Y., Shafiee, S., et al., "Adaptive nonsingular terminal sliding mode controller for micro/nanopositioning systems driven by linear piezoelectric ceramic motors," *ISA transactions*, Vol.77, pp.122-132(2018).
- Yan, G.F., "High accuracy tracking of ultrasonic motor based on PID operation of sliding surface plus inverse system compensation," *Scientific Reports*, Vol.12, No.1, pp. 1-11(2022).
- Yan, G.F., and Abidi, K., "A Practical Application of Sliding Mode Control in the Motion Control of a High Precision Piezoelectric Motor," *Journal of the Brazilian Society of Mechanical Sciences and Engineering*, Vol.44, No.5, pp.1-10(2022).
- Liang, J., Jing, K., Dong, Y., et al., "Nominal-Model-Based Sliding-Mode Control for Traveling-Wave Ultrasonic

- Motor,” *Micromachines*, Vol.13, No.11, 1846(2022).
- Bani Melhem, M. K., Simic, M., Lai, C. Y., et al., “Fuzzy control of the dual-stage feeding system consisting of a piezoelectric actuator and a linear motor for electrical discharge machining,” *Proceedings of the Institution of Mechanical Engineers, Part B: Journal of Engineering Manufacture*, Vol.234, No.5, pp.945-955(2020).
- Shi, J. Z., Huang, W. W., and Zhou, Y., “T-S Fuzzy Control of Travelling-Wave Ultrasonic Motor,” *Journal of Control, Automation and Electrical Systems*, Vol.31, No.2, pp.319-328(2020).
- Zhou, M., Wang, Y., Zhang, Y., et al., “Hysteresis inverse compensation-based model reference adaptive control for a piezoelectric micro-positioning platform,” *Smart Materials and Structures*, Vol.30, No.1, 015019(2020).
- Motoi, N., Nalbach, M., Ito, S., et al., “Adaptive Control Method Based on Recursive Least Square Method by Piezoelectric Actuator for Pulling Fibril with Parameter Variation,” *IECON 2020 The 46th Annual Conference of the IEEE Industrial Electronics Society*, IEEE, (2020).
- Yan, G.F., “Design of adaptive sliding mode controller applied to ultrasonic motor,” *Assembly Automation*, Vol.42, No.1, pp.147-154(2022).
- Li, W., Zhang, C., Gao, W., et al., “Neural network self-tuning control for a piezoelectric actuator,” *Sensors*, Vol.20, No.12, 3342(2020).
- Yan, G.F., “Inverse neural networks modelling of a piezoelectric stage with dominant variable,” *Journal of the Brazilian Society of Mechanical Sciences and Engineering*, Vol.43, No.8, pp.1-15(2021).
- Napole, C., Barambones, O., Derbeli, M., et al., “High-Performance Tracking for Piezoelectric Actuators Using Super-Twisting Algorithm Based on Artificial Neural Networks,” *Mathematics*, Vol.9, No.3, 244(2021).
- Sebastian, A., and Salapaka, S. M., “Design methodologies for robust nano-positioning,” *IEEE Transactions on Control Systems Technology*, Vol.13, No.6, pp.868-876(2005).
- Napole, C., Barambones, O., Derbeli, M., et al., “Advanced Trajectory Control for Piezoelectric Actuators Based on Robust Control Combined with Artificial Neural Networks,” *Applied Sciences*, Vol.11, No.16, 7390(2021).
- Khalil, M. M., Masuda, N., Takayama, K., et al., “A Closed-Loop Micro-Ultrasonic Motor Control System With Extremum Seeking,” *IEEE Access*, Vol.11, pp.22329-22341(2023).
- Lu, S., Shi, J. Z., “Adaptive PI control of ultrasonic motor using iterative learning methods,” *ISA transactions*, Vol.139, No.8, pp.499-509(2023).
- Zhao, L., Cai, C. C., Mao, X. F., et al., “A maximum efficiency point tracking control method for ultrasonic motors with temperature compensation,” *IET Electric Power Applications*, Vol.17, pp.1469-1477(2023).
- Parker Ltd, *Parker/Bayside Linear Stage Reference*, pp.1-19(2012).
- RGB25Y Company, *Renishaw RGB25Y Reference*, pp.1-2(2011).
- Gao, W. B., *Variable structure control theory and design method*, Press of Science, Beijing(1996).

摩擦驅動的超聲波電動機 反步趨近律控制器設計

嚴剛峰

成都大學電子資訊與電氣工程學院自動化系
貴州大學先進製造技術教育部重點實驗室

摘要

本文首先針對所選的超聲電動機控制系統建立了近似的時域數學模型，並利用最小二乘法對系統模型的參數進行了辨識。然後，針對所選超聲電動機系統提出並設計了一種反步趨近律控制器，證明了超聲電動機控制系統的穩定性，並給出了所設計控制器的參數選擇方法。最後採用大增益的比例積分微分（PID）控制方法和設計的控制方法來跟蹤同一位置信號，取得了較好的控制效果。結果表明，對於跟蹤幅度為40 mm的位置信號，PID控制方法的最大跟蹤誤差為0.1362 mm，反步趨近律控制方法的最大跟蹤誤差為0.0816 mm。相同控制參數下，添加0.3 kg的負載後，PID控制方法和反步趨近律控制方法的最大跟蹤誤差分別為0.1519 mm和0.0892 mm。所提出的控制方法易於在工程中實現，該控制方法需要調整的參數少且易於調整，因此具有良好的工程應用價值。